



A Sliding Mode approach into Constant Switching Frequency Direct Power Control of a Grid Connected Voltage Source Converter

Bechir Bouaziz, Faouzi Bacha, and Moncef Gasmi

Computer lab for industrial systems, National Institute of Applied Sciences and Technology,
Centre Urbain Nord, BP 676, 1080 Tunis Cedex, Tunisia
bechir.bouaziz@gmail.com

Abstract: This paper presents a control method which combines sliding mode approach of direct power control and operates with constant switching frequency. This novel scheme Sliding Mode Constant Switching Frequency Direct Power Control (SM-CSF-DPC) employs a nonlinear sliding mode control (SMC) approach to directly calculate the required converter's control voltage. The constant switching frequency (CSF) is achieved by using space vector modulation (SVM). In this novel scheme, the extra current control loops are eliminated, which simplifies the system design and enhances the transient performance. The improved strategy is tested on a simulation model of a two level VSC and compared with the conventional switching table direct power control (ST-DPC) strategy. The proposed SM-CSF-DPC methods have very good results both in steady-state and transients. It is shown that the proposed DPC exhibits several features, such as a simple algorithm, constant switching frequency, robust to power step change, step change of referenced DC voltage and is capable of providing enhanced transient performance in case of line voltage sags.

Index Terms: Sliding Mode Control; Direct Power Control; Voltage Source Converter; Space vector modulation

1. Introduction

The three-phase pulse width modulation (PWM) voltage source converter (VSC) has become increasingly popular in industrial applications due to its many advantages such as the bidirectional power flow, sinusoidal line current, and adjustable power factor and dc link voltage [1]. With the rapid development of renewable energy and electric power systems, such as the wind and solar power conversion, the power electronics plays a crucial role in the integration for example of the variable-speed wind power into the power system [2],[3].

The power electronic converters are used to match the characteristics of the distributed generators to such grid operation characteristics as frequency, voltage, active and reactive power, power quality, protection. In this sense it should be noticed that the introduction of power converters in a variable speed wind turbine has been mainly associated with the possibility of controlling the powers flows. The voltage source converters (VSCs) are often found in motor drivers, uninterruptible power supplies (UPS), active rectifiers and static compensators (STATCOM). VSCs are regularly used to transfer power from a DC system to an AC system or make back-to-back connection to AC systems with different frequencies such as wind turbines (WTs) and solar generation units [4],[5].

As is well-known, grid-connected voltage source converter based systems are able to control the power flow providing high efficiency and reliability levels. Generally, the control techniques which are commonly used could be classified as direct or indirect control strategies. The indirect control type Voltage Oriented Control is mainly utilized [6]. On the other hand, direct control techniques establish a direct relation between the behavior of the controlled variable and the state of the converter's switches. Direct power control (DPC) was developed for the control of grid-connected voltage-sourced converters, [7], [8].

As the grid-connected VSC is a Variable Structure System, it is a natural candidate for Sliding Mode Control (SMC). The different applications of the sliding-mode control theory

Received: February 5th, 2013. Accepted: March 10th, 2015

DOI: 10.15676/ijeei.2015.7.1.4

into the control systems of the power electronics devices have been proposed in plenty of papers [9]-[11]. The research on Sliding-Mode Control in application to the PWM rectifiers is described in [12]. The principles of Sliding-Mode Control have also been applied to design of the control systems for the active power filters [13], [14] that power circuits refer to the topology of the typical three-phase two-level PWM rectifiers. Since the Sliding-Mode Control approach has no fixed switching frequency its application to provide the PWM pattern for the power converters may result in higher level of the switching power losses. Hence the assumptions of constant frequency Sliding-Mode Control have been elaborated and applied into the switched-mode power converters including the PWM rectifiers [15]-[17].

A combination of methods and strategies results in diverse control concepts used in grid connected VSC. Such, the mixed DPC-SVM approach is an adaptation of VFOC and VF-DPC techniques, Adaptive Band Hysteresis (ABH) Current Control, sliding-control type approach is combined with predictive computing of voltage application times [18].

The contribution of this paper is to combine the conventional Switching Table based Direct Power Control (ST-DPC) strategy, sliding mode (SM) control approach and using an space vector modulation (SVM) for operated with constant switching frequency (CSF), so as to directly regulate the instantaneous active and reactive powers of grid-connected voltage source converter and controlling the dc-bus voltage.

2. Grid Connected Voltage Source Converter model

The proposed system configuration is shown in Figure 1. Considering the supply grid and the output from a three-phase voltage-sourced PWM converter as ideal voltage sources, Figure 2 shows the simplified equivalent circuit of the grid-connected bidirectional PWM converter in the stationary reference frame. According to Figure 2, the relationship between the supply, converter voltages, and line currents in the stationary reference frame is given as:

$$V_{g\alpha\beta} = R_g I_g + L_g \frac{dI_{g\alpha\beta}}{dt} + U_{g\alpha\beta} \quad (1)$$

$$C \frac{dV_{dc}}{dt} = i_{inv} - i_o = i_{inv} - (d_1 i_{g1} + d_2 i_{g2} + d_3 i_{g3})$$

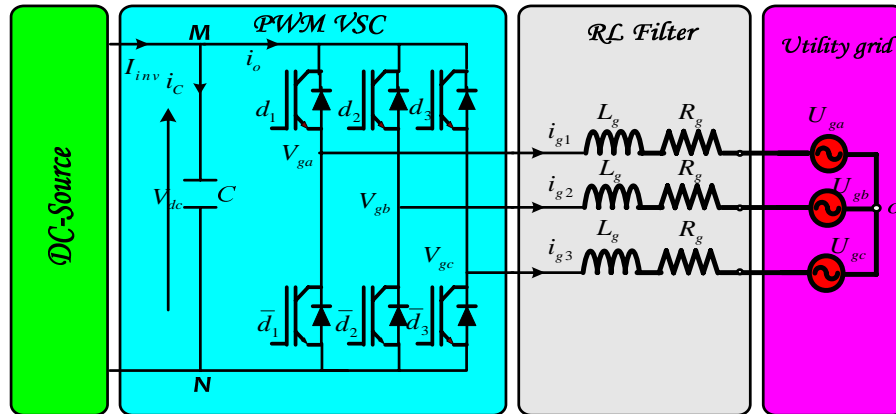


Figure 1. The PWM VSC converter placed inside the conversion chain system

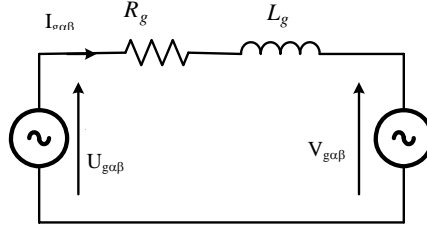


Figure 2. Equivalent circuit of the grid-connected PWM converter in the stationary frame.

In the stationary reference frame and for a balanced three-phase system, the instantaneous active and reactive power outputs, seen from the grid side, can be defined as:

$$S_g = P_g + jQ_g = -\frac{3}{2}U_{g\alpha\beta} \times I_{g\alpha\beta}^* \quad (2)$$

$$P_g = -\frac{3}{2}(u_{g\alpha}i_{g\alpha} + u_{g\beta}i_{g\beta}) \quad (3)$$

$$Q_g = -\frac{3}{2}(u_{g\beta}i_{g\alpha} - u_{g\alpha}i_{g\beta})$$

Differentiating (3) results in the instantaneous active and reactive power variations as:

$$\frac{dP_g}{dt} = -\frac{3}{2}\left(u_{g\alpha}\frac{di_{g\alpha}}{dt} + i_{g\alpha}\frac{du_{g\alpha}}{dt} + u_{g\beta}\frac{di_{g\beta}}{dt} + i_{g\beta}\frac{du_{g\beta}}{dt}\right) \quad (4)$$

$$\frac{dQ_g}{dt} = -\frac{3}{2}\left(u_{g\beta}\frac{di_{g\alpha}}{dt} + i_{g\alpha}\frac{du_{g\beta}}{dt} - u_{g\alpha}\frac{di_{g\beta}}{dt} - i_{g\beta}\frac{du_{g\alpha}}{dt}\right)$$

The line-voltage variation is also required in (5). Considering a non-perturbed line:

$$\begin{aligned} u_{g\alpha} &= U_g \sin(\omega_g t) \\ u_{g\beta} &= -U_g \cos(\omega_g t) \end{aligned} \quad (5)$$

Next instantaneous line-voltage variation law is obtained:

$$\begin{aligned} \frac{du_{g\alpha}}{dt} &= \omega_g U_g \cos(\omega_g t) = -\omega_g u_{g\beta} \\ \frac{du_{g\beta}}{dt} &= \omega_g U_g \sin(\omega_g t) = \omega_g u_{g\alpha} \end{aligned} \quad (6)$$

Based on (1), the instantaneous current variations can be expressed with respective components as

$$\begin{aligned} \frac{di_{g\alpha}}{dt} &= \frac{1}{L_g}(u_{g\alpha} - R_g i_{g\alpha} - v_{g\alpha}) \\ \frac{di_{g\beta}}{dt} &= \frac{1}{L_g}(u_{g\beta} - R_g i_{g\beta} - v_{g\beta}) \end{aligned} \quad (7)$$

It is possible to predict the power behavior knowing the instantaneous variations of the active and reactive power, which can be expressed as equations:

$$\begin{aligned} \frac{dP_g}{dt} &= -\frac{3}{2L_g}\left((u_{g\alpha}^2 + u_{g\beta}^2) - (u_{g\alpha}v_{g\alpha} + u_{g\beta}v_{g\beta})\right) - \frac{R_g}{L_g}P_g - \omega_g Q_g \\ \frac{dQ_g}{dt} &= -\frac{3}{2L_g}(u_{g\alpha}v_{g\beta} - u_{g\beta}v_{g\alpha}) - \frac{R_g}{L_g}Q_g + \omega_g P_g \end{aligned} \quad (8)$$

3. Conventional Switching Table Direct Power Control

According to the principle of conventional DPC for a three phase grid connected voltage source converter. The main idea of Switching Table based Direct Power Control (ST-DPC) was illustrated by figure 3; referenced active power P_g^{set} , delivered from outer PI DC-link voltage controller, and reactive power Q_g^{set} , set to zero for unity power factor, are compared in hysteresis controllers with estimated active and reactive powers values.

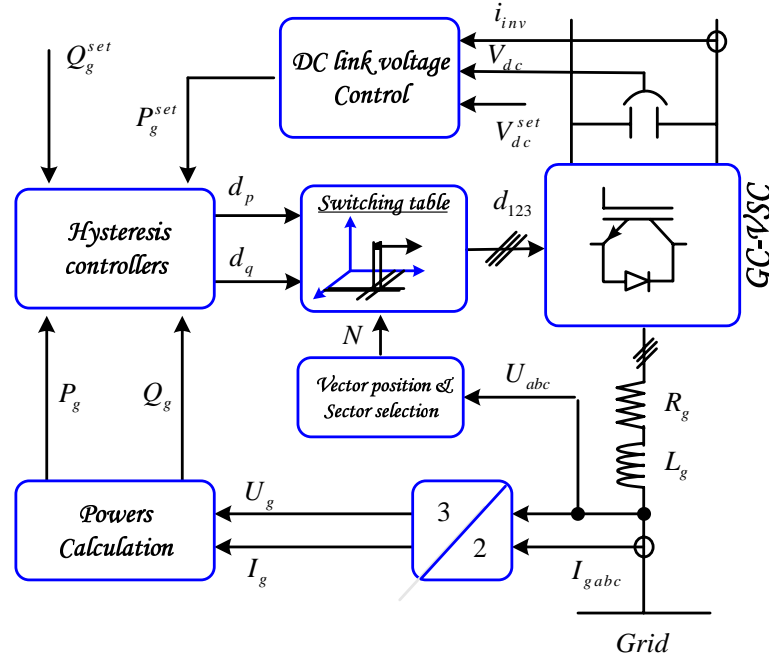


Figure 3. Control scheme of the conventional switching table direct power control (ST-DPC)

The active power digital hysteresis controller can be described as:

$$d_p = \begin{cases} 1 & \text{for } P_g < P_g^{set} - H_P \\ 0 & \text{for } P_g > P_g^{set} + H_P \end{cases} \quad (9)$$

and similarly for reactive power controller:

$$d_q = \begin{cases} 1 & \text{for } Q_g < Q_g^{set} - H_Q \\ 0 & \text{for } Q_g > Q_g^{set} + H_Q \end{cases} \quad (10)$$

Where: H_P and H_Q are hysteresis widths.

Table 1. Switching table related to line voltage vector position

States		Sector /// Voltage vector												
d _p	d _q	S 1	S 2	S 3	S 4	S 5	S 6	S 7	S 8	S 9	S1 0	S1 1	S1 2	
0	0	2	3	3	4	4	5	5	6	6	1	1	2	
0	1	7	7	8	8	7	7	8	8	7	7	8	7	
1	0	1	2	2	3	3	4	4	5	5	6	6	1	
1	1	6	1	1	2	2	3	3	4	4	5	5	6	

The $\alpha\beta$ plane is divided into twelve sectors. The relation between sectors and space vector position γ can be expressed as for line voltage space vector:

$$N_n = \left\{ \gamma \in \left[n \frac{\pi}{6}, (n+1) \frac{\pi}{6} \right] \right\} \quad (11)$$

4. Control Scheme of the proposed SM-CSF-DPC

Figure 4 shows the control scheme of proposed SM-CSF-DPC. System uses linear PI controller in outer DC-link voltage stabilization loop, which produces active power reference for the active power controller. Instantaneous active and reactive powers are calculated on the basis of line voltages, and line currents measurement. The developed SM-CSF-DPC strategy is capable of directly generating converter voltage reference in the stationary reference frame according to the instantaneous active and reactive power errors. Accordingly, the required converter's voltage $V_{g\alpha\beta}$, calculated from (20) as the input to space vector modulation (SVM) module.

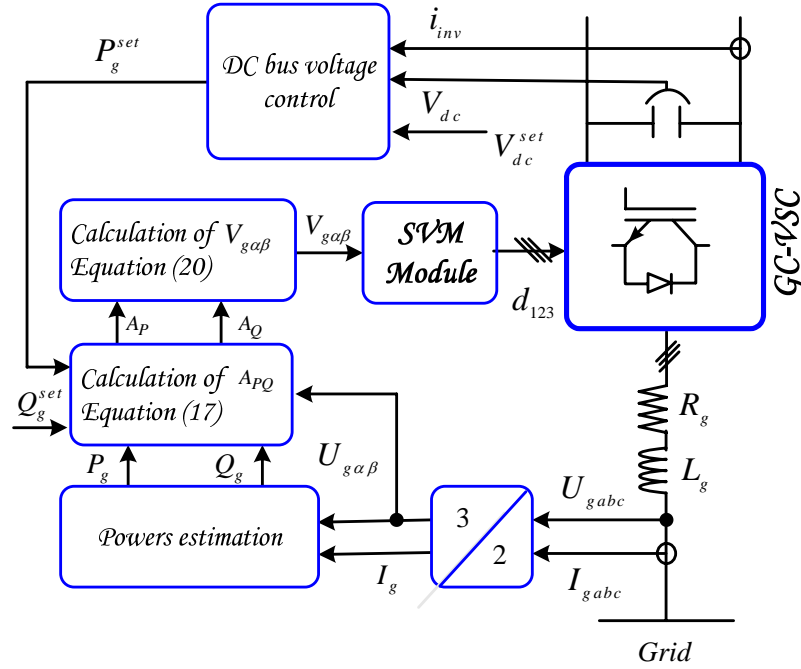


Figure 4. Control scheme of the sliding mode constant switching frequency direct power control (SM-CSF-DPC)

The design of the sliding mode control supports the problems of stability and the desired performance in a systematic way. The implementation of this control method is performed in three main steps. A SMC approach is proposed and designed for grid-connected dc/ac converters in the following section.

A. Sliding surface

The core of the design of the Sliding-Mode Control system is the definition of the sliding surface which is the track to be mapped by the system trajectory while converging towards the origin. In order to maintain the enhanced transient response and minimize the steady-state error, the switching surfaces can be in the integral forms and defined by:

$$\begin{aligned} S_P &= e_P + \lambda_P \int_0^t e_P(t) dt - e_P(0) \\ S_Q &= e_Q + \lambda_Q \int_0^t e_Q(t) dt - e_Q(0) \end{aligned} \quad (12)$$

Where $e_P = P_g^{set} - P_g$ and $e_Q = Q_g^{set} - Q_g$ are the respective errors between the sets values and the actual values of instantaneous active and reactive powers. λ_P and λ_Q are the positive control gains.

Since it is necessary that the system trajectories in the vicinity of the sliding surface $s(x)=0$ are oriented towards it, the sufficient condition for the sliding-mode existence can be derived from the equations:

$$\begin{aligned} \dot{e}_P &= -\lambda_P e_P(t) \\ \dot{e}_Q &= -\lambda_Q e_Q(t) \end{aligned} \quad (13)$$

B. Design of the control law

In the sliding mode control law design, the task is to force the system state trajectory to the interaction of the switching surfaces.

$$\begin{aligned} \dot{S}_P &= \dot{e}_P + \lambda_P e_P = -\dot{P}_g + \lambda_P e_P \\ \dot{S}_Q &= \dot{e}_Q + \lambda_Q e_Q = -\dot{Q}_g + \lambda_Q e_Q \end{aligned} \quad (14)$$

Substituting (8) into (14) leads to

$$\dot{S} = A + BV_g \quad (15)$$

Where:

$$[S_P \ S_Q]^T, A = [A_P \ A_Q]^T, V_g = [v_{g\alpha} \ v_{g\beta}]^T, B = -\frac{3}{2L_g} \begin{bmatrix} u_{g\alpha} & u_{g\beta} \\ u_{g\beta} & -u_{g\alpha} \end{bmatrix} \quad (16)$$

The expressions of the quantities A_P and A_Q are given by:

$$\begin{aligned} A_P &= \frac{3}{2L_g} (u_{g\alpha}^2 + u_{g\beta}^2) + \frac{R_g}{L_g} P_g + \omega_g Q_g + \lambda_P e_P \\ A_Q &= \frac{R_g}{L_g} Q_g - \omega_g P_g + \lambda_Q e_Q \end{aligned} \quad (17)$$

Let us consider the following quadratic Lyapunov function:

$$W = \frac{1}{2} S^T S \quad (18)$$

The time derivative of the quadratic Lyapunov function is then given by:

$$\frac{dW}{dt} = S^T \frac{dS}{dt} = S^T (A + BV_g) \quad (19)$$

The switch control law must be properly chosen so that the time derivative of quadratic Lyapunov function is definitely negative with $S \neq 0$. Therefore, the following control law is selected

$$\begin{bmatrix} v_{g\alpha} \\ v_{g\beta} \end{bmatrix} = -B^{-1} \left\{ \begin{bmatrix} A_P \\ A_Q \end{bmatrix} + \begin{bmatrix} \lambda_{P1} & 0 \\ 0 & \lambda_{Q1} \end{bmatrix} \begin{bmatrix} \text{sgn}(S_P) \\ \text{sgn}(S_Q) \end{bmatrix} \right\} \quad (20)$$

The constant switching frequency (CSF) is achieved by using space vector modulation (SVM) and the sliding mode control scheme is suggested to generate the converter output voltage reference as the input to SVM module.

C. Space vector modulation

The SVM bases on vector representation and the proportional selection of converter available states during the switching period. In two-level converter there are six active vectors and two zero vectors shown in Figure 5 to choose from. The states are the same as in the case of six-step modulation. The main idea behind SVM is that it uses formula to calculate timing of active and zero vectors. The t_1 and t_2 are the duration time of two neighbor's active states in given sector, the rest of the time t_0 is used for zero vectors.

From Figure 5, the switching time duration can be calculated as follows:

$$t_1 = \frac{\sqrt{3}T_{sw}V_{ref}}{V_{dc}} \sin\left(\frac{\pi}{3} - \theta\right) \quad (21)$$

$$t_2 = \frac{\sqrt{3}T_{sw}V_{ref}}{V_{dc}} \sin(\theta) \quad (22)$$

$$t_0 = T_{sw} - t_1 - t_2 \quad (23)$$

Where: T_{sw} is the switching period

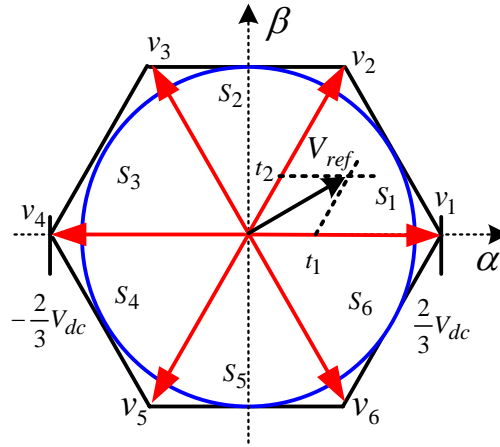


Figure 5. Space vector diagram of the two level voltage source converters (2L-VSC)

The maximum magnitude of the reference vector V_{ref} corresponds to the radius of the largest circle inscribed within the hexagon shown in Figure 5. Since the hexagon is formed by

six active vectors having a length of $\frac{2V_{dc}}{3}$, the maximum reference can be found as:

$$V_{ref \max} = \frac{V_{dc}}{\sqrt{3}}$$

Therefore, space vector modulation can be implemented by three steps. The first is to calculate the current sector and angle inside it. Based on the angle in the range of first sector the proportion of two active and one zero-vector is calculated as t_1, t_2 and t_0 . Finally, the determination of switching time of each transistor.

D. Chattering phenomenon

The chattering phenomenon cannot be uniquely claimed as a desirable or undesirable effect. It results naturally from the introduction of the discontinuous control signal which gain is usually constant but its sign is being switched non uniformly during the control process. There are several techniques of the chattering suppression reported in literature on Sliding-Mode Control. The following section introduces the method chattering suppression techniques. The most common method is boundary layer solution. As a result, a continuous function around the sliding surface neighborhood is obtained as

$$\text{sgn}(S_j) = \begin{cases} 1 & \text{if } S_j > \phi_j \\ \frac{S_j}{D_j} & \text{if } |S_j| \leq \phi_j \\ -1 & \text{if } S_j < -\phi_j \end{cases} \quad (26)$$

Where ϕ_j is the width of the boundary layer and j represents active and reactive powers respectively

E. Proof of the Stability

For the stability against sliding surfaces, it is sufficient to satisfy the stability condition $\dot{W} < 0$. By setting appropriate switch functions, stability can be achieved and formulated by the following condition

$$\text{If } \begin{cases} S_P \text{sgn}(S_P) > 0 \\ S_Q \text{sgn}(S_Q) > 0 \end{cases} \quad \text{then} \quad \dot{W} = S^T \dot{S} = -S^T \begin{bmatrix} \lambda_{P1} & 0 \\ 0 & \lambda_{Q1} \end{bmatrix} \begin{bmatrix} \text{sgn}(S_P) \\ \text{sgn}(S_Q) \end{bmatrix} \quad (24)$$

F. Proof of the Robustness

The most distinguish property of the variable structure control is the ability to provide the robustness to parametric uncertainty and external disturbances. The sliding surface will be affected by these disturbances. Thus, (15) should be rearranged as

$$\dot{S} = A + BV_g + D \quad (25)$$

Where $D = [D_P \quad D_Q]$ represents system disturbances.

5. Simulation Results and Discussion

In order to verify developed control methods, several simulations have been carried out. Control strategies have been tested under steady state and transient conditions. The basic simulation parameters have been listed in table 2 and table 3.

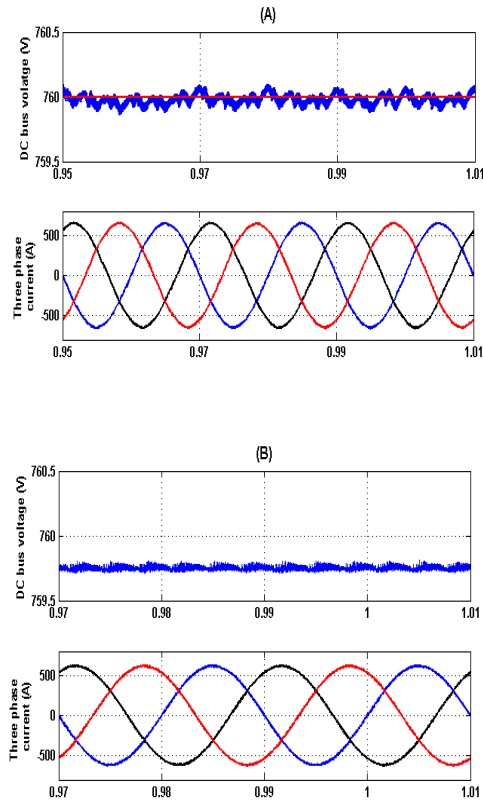
Table 2 . Parameters of the tested PWM VSC converter system

Parameters	Values
Rated power (kW)	300
Dc-bus voltage (V)	760
Dc-bus capacitor (mF)	100
Filter resistance (mohms)	5
Filter inductance (mH)	0.5
AC supply frequency (Hz)	50
Line to line ac voltage (V)	400

Table 3. Control parameters of SMC approach

Parameters	Values
Positive gains λ_P and λ_Q	2500
Control gains λ_{P1} and λ_{Q1}	10^7
Width of boundary layout ϕ_P and ϕ_Q	400/200

A. Steady State Operation



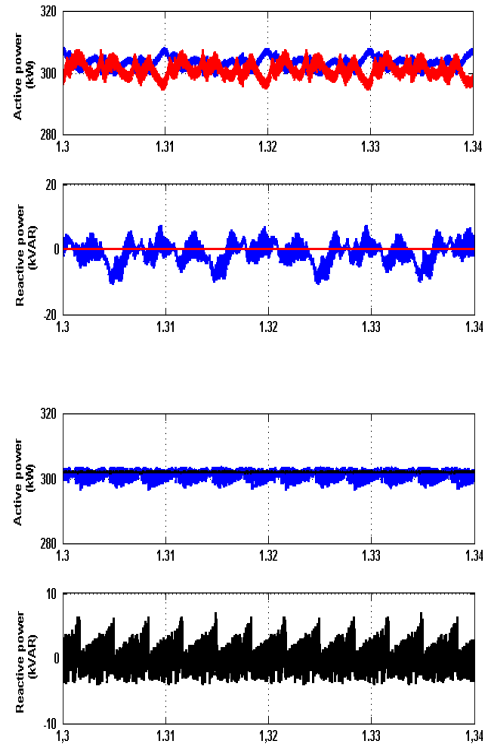


Figure 6. Steady state operation of (A) CSF-ST-DPC and (B) ST-DPC

Proposed control methods have been compared under steady state operation. To investigate the DC voltage control loop, all tests have been carried out with closed control loop, and under unity power factor condition $Q_g^{set} = 0$. The reference value of active power P_g^{set} has been set to 300 kW and the set value of DC bus voltage has been set to 760 V.

Figure 6(A and B) show the steady state operation for the two level voltage source converter (2L-VSC), using both those ST-DPC and CSF-ST-DPC control strategies. As can be observed the CSF-ST-DPC shows the best power quality (THDi=2.75%) and the minimum power ripple. The ST-DPC leads to a dispersed harmonic spectrum with a large THD of around 3.79% with considerable power ripple.

On the other hand, the CSF-ST-DPC shows a small tracking error, while the absolute tracking error in the ST-DPC case is large. Furthermore, the voltage ripple in the DC-link capacitor is clearly smaller with excellent closed loop control in the CSF-ST-DPC than the ST-DPC strategy.

Figure 7 shows converter voltage measured between converter phase (a) input and negative DC bus as well as related number of transistor “on” and “off” switching per one cycle. For CSF-ST-DPC constant number of switching is ensured by Space Vector Modulator (SVM)

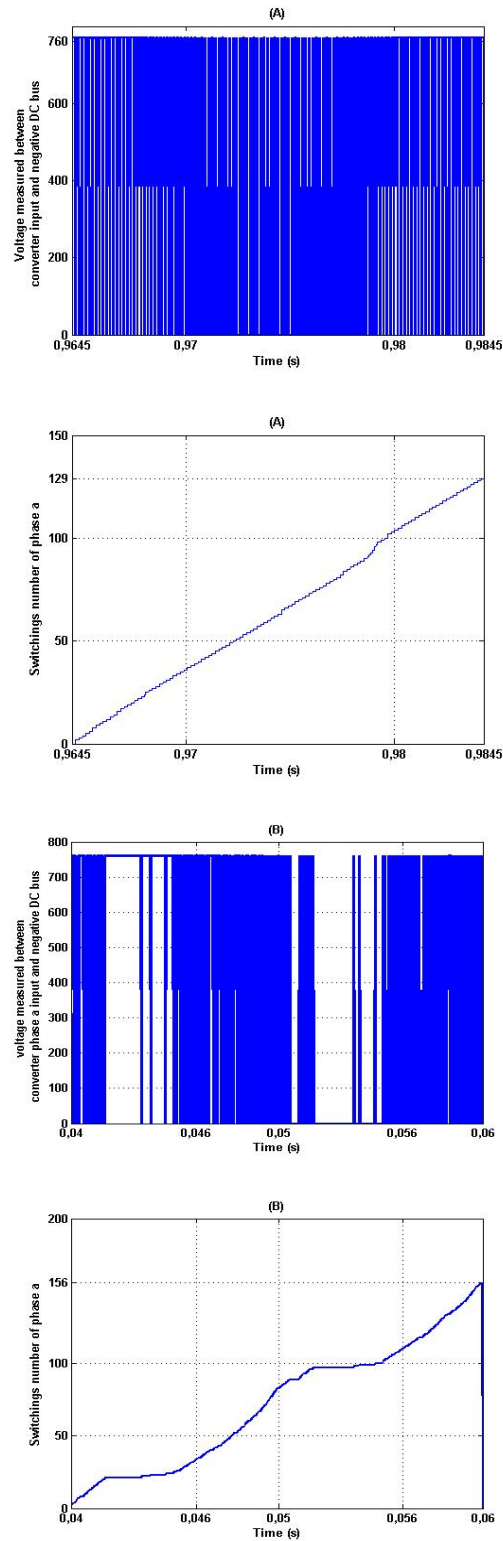


Figure 7. Switching's number and voltage measured between converter input and negative DC bus in phase a. (A) CSF-ST-DPC, (B) ST-DPC.

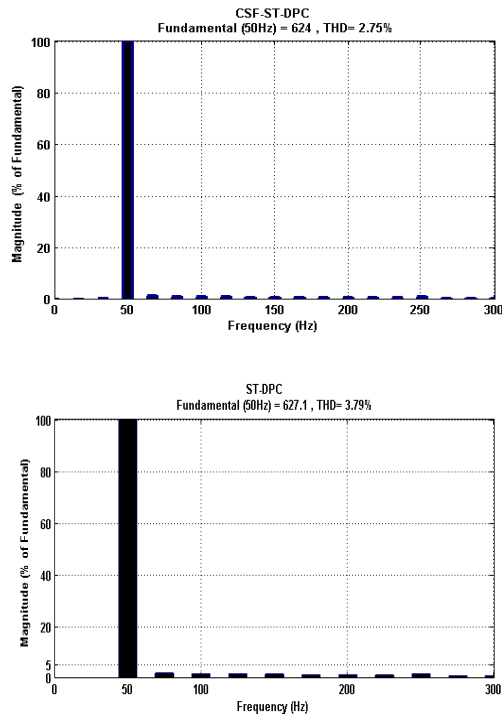


Figure 8. Line current harmonics spectrum

B. Transient Operation

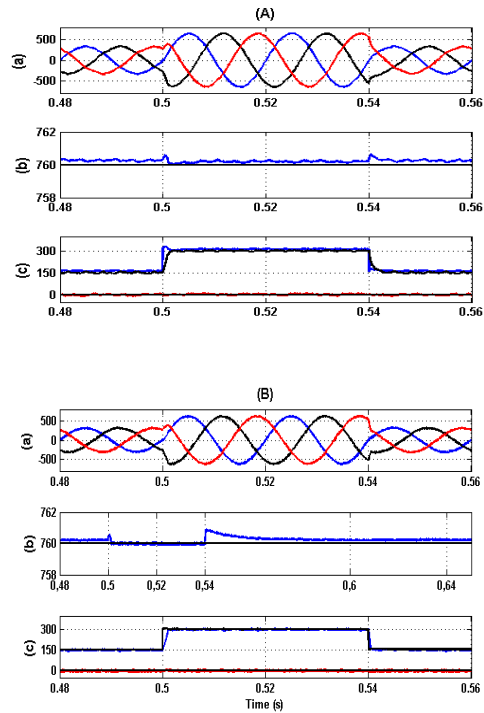


Figure 9. Transient operation of (A) CSF-ST-DPC and (B) ST-DPC power step change from 150 kW to 300 kW: (a) line currents (A), (b) DC link voltage (V), (c) referenced and measured active and reactive power

Behavior of presented control methods have been compared under transient states. Figure 9 shows the first test was step change of referenced active power P_g^{set} from 150 kW to 300 kW, and has been carried out with closed DC-link voltage control loop.

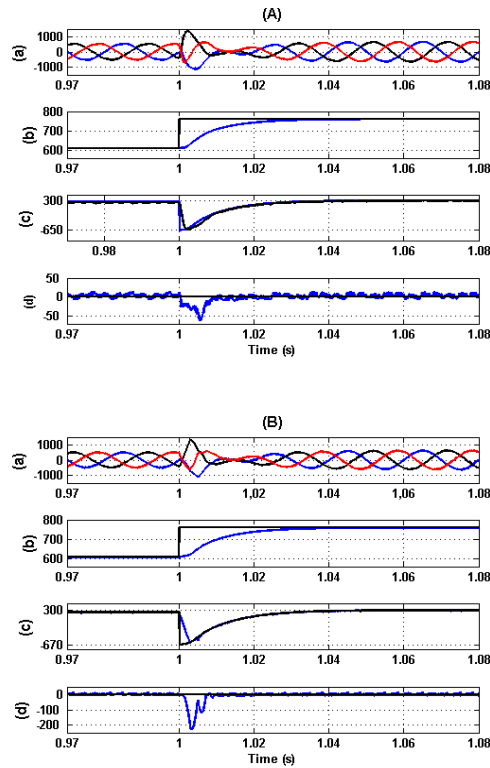


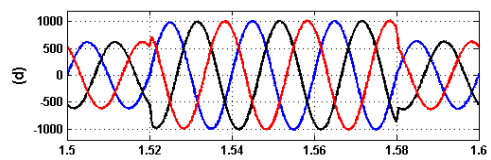
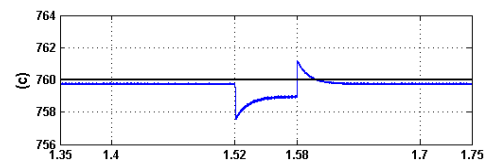
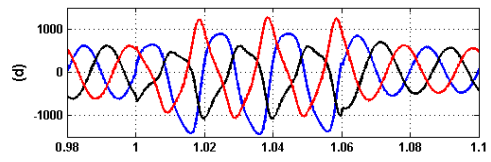
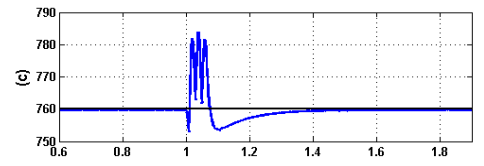
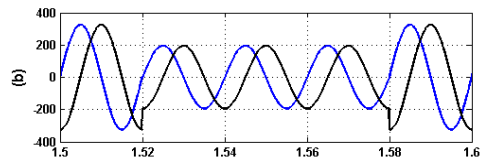
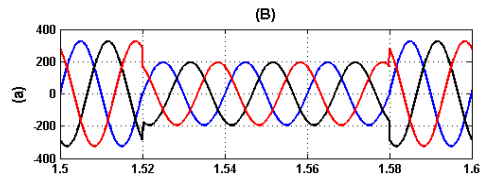
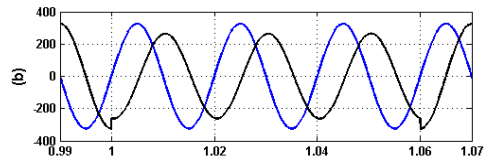
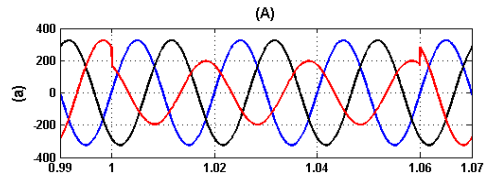
Figure 10. Transient operation of (A) CSF-ST-DPC and (B) ST-DPC step change of referenced DC voltage from 600 V to 760 V: (a) line currents (A), (b) DC link voltage (V), (c) referenced and measured active, (d) referenced and measured reactive power

Figures 10 present second tests, which was step change of DC-link voltage reference value from 600 V to 760 V. As shown Figure 9-10, the CSF-ST-DPC is clearly faster than the ST-DPC in power tracking task. The proposed scheme presents superiority in terms of a setting time, rise time and overshoot. Furthermore, there is no ripple of active and reactive power in the CSF-ST-DPC, whereas the ST-DPC shows a substantial perturbation in the reactive power behavior when active power changes are applied.

Connections and disconnections of large loads, and short circuits in the system can cause line voltage sags; it's the sudden drop of line voltage value. The influence of Line Voltage Sags operation of CSF-ST-DPC and ST-DPC approach under single and three phase voltage sags will be investigated.

Figure 11 shows operation under line voltage sags. As it can be seen, line voltage sag, causes DC-link voltage drop. Next, DC-link voltage controller, trying to keep the set value of DC bus voltage.

In the CSF-ST-DPC algorithm, the line voltage sag directly leads to a proportional increase of line current in order to keep the power requirements constant. Figure 11 (A) shows the line-phase estimation of the CSF-ST-DPC algorithm in the presence of a three-phase voltage sag between 1.52s and 1.58s. This control algorithm shows a similar behavior which is coherent with the fact that the three-phase balance is kept during the voltage drop.



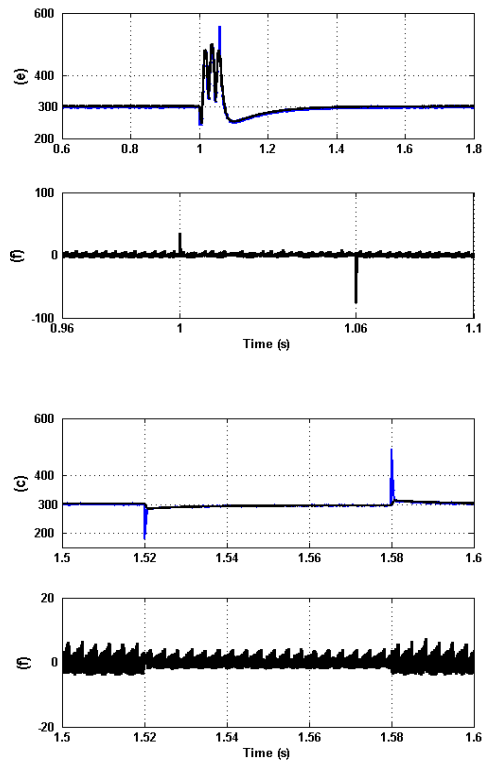


Figure 11. Operation under voltage sags: (A) single phase sag, and (B) three phase sags

6. Conclusion

This paper has presented a sliding mode approach of direct power control for a Grid connected voltage source converter and operates with constant switching frequency using space vector modulation. The CSF-ST-DPC strategy, based on sliding mode control approach combined to conventional switching table DPC and space vector modulation module. System responses with the proposed CSF-SM-DPC method are validated via both simulations and compared with of conventional ST-DPC strategy. Simulation results confirm that the proposed strategy is more robust to step power variations and voltage sags operation than the conventional one do. The pretty well features of the proposed CSF-SM-DPC strategy are the excellent transient performance and the steady-state responses under the disturbances.

7. References

- [1] Hu, J., He, Y. "Modeling and control of grid-connected voltage-sourced converters under generalized unbalanced operation conditions". *IEEE Trans. Energy Conv*, vol.23, No.3, 903-913, 2008.
- [2] J. M. Carrasco et al, "Power Electronic Systems for the Grid Integration of Renewable Energy Sources: A Survey", *IEEE Trans. Ind. Electron*, Vol. 53, No. 4, pp. 1002 – 1016, August 2006.
- [3] Z. Chen, I. M. Guerrero and F. Blaabjerg, "A review of the State of the Art of Power Electronics for Wind Turbines", *IEEE Trans. on Power Electronics*, Vol. 24, No. 8, pp. 1859 – 1875, August 2009.
- [4] J. Rodriguez, I. Dixon, J. Espinoza and P. Lezana, "PWM Regenerative Rectifiers: State of the Art", *IEEE Trans. on Industrial Electronics*, Vol.52, No.1, pp. 5 – 22, February 2005.

- [5] H. Abu-Rub, I. Holtz, J. Rodriguez and G. Baoming, “Medium-Voltage Multilevel Converters-State of the Art, Challenges, and Requirements in Industrial Applications”, *IEEE Trans. Ind. Electron*, Vol. 57, No. 8, pp. 2581 – 2596, August 2010.
- [6] M. Malinowski, M. Jasinski and M. P. Kazmierkowski: “Simple Direct Power Control of Three-Phase PWM Rectifier Using Space-Vector Modulation (DPC-SVM)”, *IEEE Trans. Ind. Electron*, Vol. 51, No. 2, pp. 447-454. April 2004.
- [7] D. Zhi, L. Xu, and B. W. Williams, “Improved direct power control of grid-connected DC/AC converters,” *IEEE Trans. Power Electron.*, vol. 24,no. 5, pp. 1280–1292, May 2009.
- [8] S. Aurtenechea, M. A. Rodriguez, E. Oyarbide, and J. R. Torrealday, “Predictive control strategy for DC/AC converters based on direct power control,” *IEEE Trans. Ind. Electron.*, vol. 54, no. 3, pp. 1261–1271, Jun. 2007.
- [9] Benchaib A., Rachid A., Audrezet E., Tadjine M., “Real-Time Sliding-Mode Observer and Control of an Induction Motor”, *IEEE Transactions on Industrial Electronics*, vol.46, no.1, February 1999, pp.128-138.
- [10] Mazumder S.K., “A Novel Discrete Control Strategy for Independent Stabilization of Parallel Three-Phase Boost Converters by Combining Space-Vector Modulation With Variable Structure Control”, *IEEE Transactions on Power Electronics*, vol.18, no.4, July 2003, pp.1070-1083.
- [11] Mazumder S. K., “Continuous and Discrete Variable-Structure Controls Strategy for Parallel Three-Phase Rectifier”, *IEEE Transactions on Industrial Electronics*, vol.52, no.2, April 2005, pp.340-354.
- [12] Sabanovic N., Sabanovic A., Ohnishi K., “Sliding Modes Control Three-Phase Switching Power Converters”, 18th *International Conference on Industrial Electronics, Control and Instrumentation IECON*, November 1992, pp.319-324.
- [13] Soares V., Verdelho P., Marques G. D., “An Instantaneous Active and Reactive Current Component Method for Active Filters”, *IEEE Transactions on Power Electronics*, vol.15, no.4, July 2000, pp.660-669.
- [14] Pires V. F., Silva J. F., “A Current Source Active Power Filter Controlled by a Sliding Mode Approach”, 12th *International Power Electronics and Motion Control Conference EPE-PEMC*, 2006, pp.1654-1659.
- [15] Pinto S. F., Silva J. F., “Constant-Frequency Sliding-Mode and PI Linear Controllers for Power Rectifiers: A Comparison”, *IEEE Transactions on Industrial Electronics*, vol.46, no.1, February 1999, pp.39-51.
- [16] M. Malinowski, M. P. Kazmierkowski and A. M. Trzynadlowski, “A Comparative Study of Control Techniques for PWM Rectifiers in AC Adjustable Speed Drives”, *IEEE Trans. Power Electron*, Vol. 18, No. 6, November 2003
- [17] M. Malinowski et al, “Virtual-Flux-Based Direct Power Control of Three-Phase PWM Rectifiers”, *IEEE Trans. on Ind. Applications*, Vol. 37, No. 4, July/August 2001
- [18] A. Sarinana, S. Guffon, G. Bornard, and S. Bacha, “A novel fixed switching frequency controller of a three-phase voltage source inverter”, in 8th *European Conference on Power Electronics and Applications*. EPE, pp. 9, 1999.



Bechir BOUAZIZ was born in Gabes, Tunisia 1985. He received his diploma in electrical engineering from the High Technical and Science School in Tunis (ESSTT), university of Tunis, Tunisia in June 2008. He also received his master thesis degree in electrical engineering on June 2010. He is currently doing his PhD thesis researches in the theme of advanced control strategies for wind energy. Mr BOUAZIZ had worked in the LISI team of renewable energy and is actually working in the research team development of advanced wind system's control.



Faouzi BACHA was born in Ben Guerdanne, Tunisia in 1964. He received "Habilitation Universities" in electrical engineering on 2008 from the National Institute of electric engineering (ENIT), Tunisia. He is currently an associate Professor at the High Technical and Science School (ESSTT) in Tunis, Tunisia. He has numerous publications on direct control of synchronous and induction machines. His research fields include modeling and simulation of electrical machines, power system and wind energy. Dr Bacha is a member of working group on wind energy application in Tunisia.



Moncef GASMI was born in Tunis, Tunisia, in 1958. He received respectively, from the Tunis National School of Engineering (ENIT), the Principal Engineering Diploma in Electrical Engineering in 1984, the Master of Systems Analysis and Computational Treatment in 1985, the Doctorate in Automatic Control in 1989 and the State Doctorate in Electrical Engineering in 2001. Now, he is Professor and Director of the Computer lab for Industrial Systems (CLIS) at the National Institute of Applied Sciences and Technology (INSAT). His domain of interests is related to the modeling, analysis and control of complex systems.